

# IMPROVED DISPLACEMENT CROSS SECTIONS FOR STRUCTURAL MATERIALS IRRADIATED WITH INTERMEDIATE AND HIGH ENERGY PROTONS

A.Yu.Konobeyev, C.H.M.Broeders, U.Fischer

*Institut für Reaktorsicherheit, Forschungszentrum Karlsruhe GmbH, Herrmann-von-Helmholtz-Platz 1, Eggenstein-Leopoldshafen 76344 Germany, konobeev@irs.fzk.de, broeders@irs.fzk.de, fischer@irs.fzk.de*

*Displacement cross-sections were calculated for iron, copper, and tungsten at incident proton energies from several keV up to 100 GeV. Recoil energy distributions were obtained using various approaches including the nuclear optical model and the intranuclear cascade evaporation model. The number of defects was calculated using the binary collision approximation model and results of molecular dynamics simulations. Obtained displacement cross-sections are compared with available experimental data.*

## I. INTRODUCTION

Traditionally, the NRT model<sup>1,2</sup> is used for the calculation of displacement cross-sections for structural materials. Its relative simplicity and implementation in popular codes (NJOY, MCNPX, SPECTER) allows to perform the quick evaluation of the number of defects produced under the irradiation. At the same time, available experimental data<sup>3</sup> and more rigorous calculations show the difference with NRT evaluations. It makes essential the calculation of displacement cross-sections for structural materials using advanced models, which predictions are close to available measured data.

The goal of this work is the calculation of displacement cross-sections for a number of structural materials in a wide energy range of primary protons. The number of defects produced by primary knock on atoms (PKA) in materials is calculated with the help of the binary collision approximation model (BCA) using the results obtained by the method of the molecular dynamics (MD). Calculations of primary recoil spectra are performed using various models, including the optical model and different versions of intranuclear cascade evaporation model.

## II. THE METHOD USED FOR DISPLACEMENT CROSS-SECTION CALCULATIONS

The total value of the displacement cross-section is calculated as the sum of the proton elastic displacement

cross-section  $\sigma_{d,el}$  and the displacement cross-section for proton nonelastic interactions  $\sigma_{d,non}$ .

The general formula for the calculation of the displacement cross-section is as follows

$$\sigma_d(E_p) = \sum_i \int_{E_d}^{T_i^{\max}} d\sigma(E_p, Z_T, A_T, Z_i, A_i, T_i) / dT_i \times v(T_i, Z_T, A_T, Z_i, A_i) dT_i \quad (1)$$

where  $E_p$  is the incident proton energy;  $d\sigma/dT_i$  is the recoil atom energy distribution;  $Z_T$  and  $A_T$  are the atomic number and the mass number of the target, correspondingly;  $Z_i$  and  $A_i$  are the same for the recoil atom (for the elastic scattering  $Z_i = Z_T$ ,  $A_i = A_T$ );  $v(T_i)$  is the number of Frenkel pairs produced by PKA with the kinetic energy  $T_i$ ,  $T_i^{\max}$  is the maximal kinetic energy of the PKA produced in  $i$ -th reactions; the summation is over all recoil atoms produced in the irradiation.

The number of defects produced in irradiated material is calculated as follows

$$v(T_i) = \eta \cdot N_{NRT}, \quad (2)$$

where  $N_{NRT}$  is the number of defects predicted by NRT<sup>1,2</sup>:  $N_{NRT} = 0.8 \cdot T_{dam} / (2E_d)$ ;  $T_{dam}$  is the “damage energy” equal to the energy transferred to lattice atoms reduced by the losses for electronic stopping of atoms in the displacement cascade;  $\eta$  is the defect production efficiency<sup>3</sup>;  $E_d$  is effective threshold displacement energy.

### I.A. Calculation of the Number of Displacements in Irradiated Materials

For an ion moving in the material the simulation of atomic collisions was performed by BCA up to a certain minimal “critical” energy ( $T_{crit}$ ) of the ion. Below this energy the BCA calculation was interrupted and the number of defects was estimated using results of MD simulations. The procedure was performed for all PKAs formed in atomic collision cascades<sup>4,5</sup>.

The number of Frenkel pairs created by ions with the energy below  $T_{\text{crit}}$  has been estimated according to empirical equations for the defect production efficiency obtained in Refs. 6, 7, and 8, which approximate results of the MD simulation

iron<sup>6,7</sup>:

$$\eta = 0.5608T_{\text{dam}}^{-0.3029} + 3.227 \times 10^{-3} T_{\text{dam}}, \quad (3)$$

copper<sup>8</sup>:

$$\eta = 0.7066T_{\text{dam}}^{-0.437} + 2.28 \times 10^{-3} T_{\text{dam}}, \quad (4)$$

tungsten<sup>8</sup>:

$$\eta = 1.0184T_{\text{dam}}^{-0.667} + 5.06 \times 10^{-3} T_{\text{dam}}, \quad (5)$$

where  $T_{\text{dam}}$  is taken in keV and it is supposed that the initial energy in the MD simulation is close to the damage energy.

The use of Eq.(3)-(5) is justified up to a certain maximal damage energy  $T_{\text{dam}}$ , which is shown in Table I together with the corresponding critical energy. The same  $T_{\text{dam}}$  value has been used in the present work for the transition from MD to BCA calculations.

TABLE I. The critical energy (kinetic energy of ion) and the corresponding damage energy for the self-ion irradiation of iron, copper and tungsten

Material	$T_{\text{crit}}$ (keV)	$T_{\text{dam}}$ (keV)
Iron	61.2	40
Copper	28.3	20
Tungsten	40.8	31

Numerical calculations of the number of defects produced by ions in materials were performed using the IOTA code<sup>9</sup>.

The ratio of calculated number of displacements  $v(T)$  to the  $N_{\text{NRT}}$  value (efficiency of the defect generation, Eq.(2)) is shown in Fig.1 for the Cu-Cu irradiation<sup>10</sup> and in Fig.2 for W-W irradiation. The value of the efficiency  $\eta$  is shown as a function of the damage energy  $T_{\text{dam}}$  in the energy range which corresponds to the primary kinetic energy of Cu- and W- ions up to 5.0 GeV. Values of  $E_d$  adopted for copper and tungsten are equal to 30 eV and 90 eV correspondingly. The result of the joint BCA-MD simulation for self-ion irradiation of iron is demonstrated in Ref.11.

Presumably, the growth of the defect production efficiency at energies  $T_{\text{dam}}$  above  $\sim 20$  keV (Fig.1,2). results from the decrease of the averaged energy transferred in ion-ion collision with the increase of the projectile energy. Small energies correspond to the part of  $\eta(T_{\text{dam}})$  (Fig.1,2) with a relatively high values of  $\eta$ .

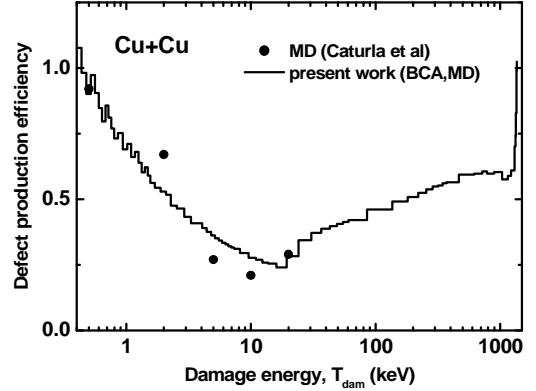


Fig. 1. The efficiency of the defect production for the Cu-Cu irradiation obtained using the combined BCA-MD method<sup>10</sup> (histogram) and results of the MD simulation<sup>8</sup> (dots).

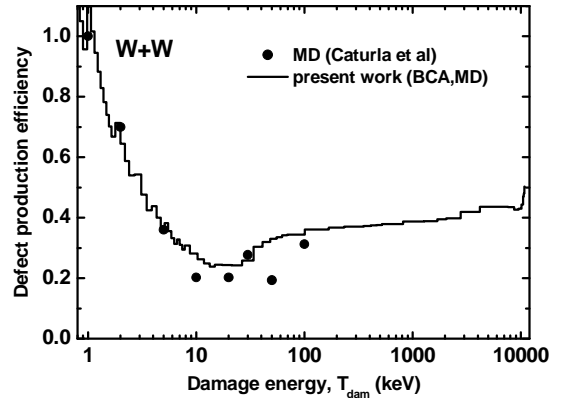


Fig. 2. The efficiency of the defect production for the W-W irradiation obtained using the combined BCA-MD method (histogram) and results of the MD simulation<sup>8</sup> (dots).

## I.B. Elastic Proton Scattering

The correct description of the recoil energy distribution in the proton elastic interactions with atoms includes the consideration of the screened Coulomb scattering in material, the nuclear scattering and their interference.

At the proton incident energy below 1 MeV the screening effect plays an important role in the proton elastic scattering on atoms. The recoil energy distribution can be written in the following form

$$d\sigma(E_p, T) = \pi a^2 f(t^{1/2}) \frac{dt}{2t^{3/2}}, \quad (6)$$

where the  $f(t^{1/2})$  is the screening function<sup>12-15</sup>, “ $a$ ” is the screening length, and “ $t$ ” is the reduced energy.

Fig.3 illustrates the difference of  $\sigma_{d,el}$  values calculated using various screening functions for copper. It shows the ratio of elastic displacement cross-sections obtained using  $f(t^{1/2})$  from Refs.12, 14, and 15 to  $\sigma_{d,el}$  calculated using the screening function from Ref.13.

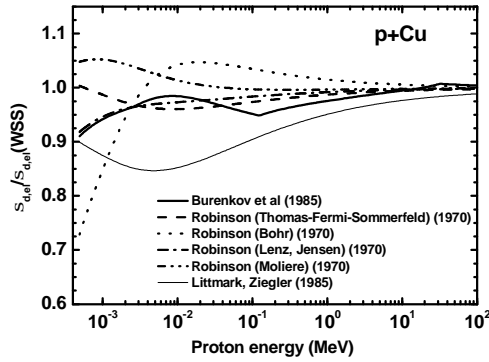


Fig. 3. The ratio of proton elastic displacement cross-sections obtained using various screening functions<sup>12,14,15</sup> to the elastic displacement cross-section calculated using  $f(t^{1/2})$  from Ref.13 for copper.

The contribution of the nuclear scattering in the recoil energy distribution becomes appreciable for the  $\sigma_{d,el}$  calculation at energies above  $\sim 5$  MeV, where the screening effect is small. It allows applying the nuclear optical model for elastic displacement cross-section calculations (see details in Refs. 4,10).

Fig.4 shows the proton elastic displacement cross-section for tungsten at the energy range from several keV up to 100 GeV. The  $d\sigma(E_p, T)$  has been calculated using Eq.(6) with  $f(t^{1/2})$  from Ref.13 for the proton energy up to 2.5 MeV, the optical model with parameters from Ref.16 up to the proton energy 50 MeV and optical model parameters from Ref.17 up to  $E_p=0.4$  GeV, and using the relativistic formula from Ref.18. The  $\sigma_{d,el}$  values for copper are discussed in Ref.10.

### I.C. Nonelastic Proton Interactions with Nuclei

#### I.C.1. Calculation of the number of defects using combined BCA-MD approach

To calculate the value of the displacement cross-section for nonelastic proton interactions with atoms ( $\sigma_{d,non}$ ) collision cascades were simulated for all residual atoms produced in nuclear reactions induced by primary protons using the method described in Section I.A.

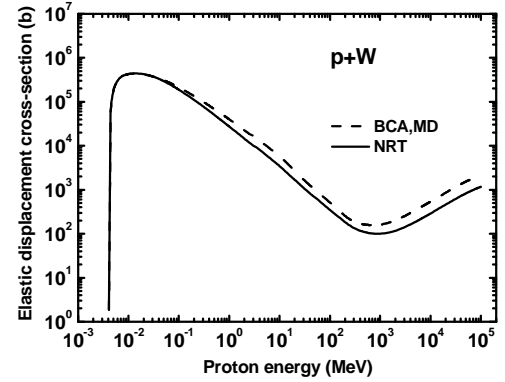


Fig. 4. Displacement cross-section for elastic proton interactions with natural tungsten calculated using the combined BCA-MD method (solid line) and the NRT model (dashed line).

Calculations of recoil energy distributions were performed using various nuclear models implemented in MCNPX<sup>19</sup>, CASCADE<sup>20</sup>, and DISCA-C<sup>21,22</sup> codes. The number of defects has been calculated by the BCA-MD approach using the IOTA code<sup>9</sup>.

Examples of displacement cross-sections calculated for the proton nonelastic interaction with <sup>184</sup>W at various incident energies are shown in Tables II-V. Data for copper are discussed in Ref.10.

TABLE II. Displacement cross-sections (b) for nonelastic interactions of 20 MeV- protons with <sup>184</sup>W. The nonelastic cross-section is equal to 1.465 b.

Nuclear model	BCA-MD	NRT
CEM03	219	550
DISCA-C	231	577
Average value	225	564

TABLE III. Displacement cross-sections (b) for nonelastic interactions of 150 MeV- protons with <sup>184</sup>W. The nonelastic cross-section is equal to 1.64 b.

Nuclear model	BCA-MD	NRT
Bertini/Dresner	982	2460
Bertini/ABLA	1070	2660
ISABEL/Dresner	925	2330
ISABEL/ABLA	1020	2540
CEM03	879	2220
INCL4/Dresner	886	2260
INCL4/ABLA	957	2420
FLUKA/Dresner	1080	2720
FLUKA/ABLA	1160	2900
CASCADE	1070	2660
DISCA	932	2360
Average value	997 ± 91	2500 ± 210

There is a significant scattering of displacement cross-sections calculated using various nuclear models (see Tables II-V and Ref.10). An accurate evaluation of  $\sigma_{d,non}$  can be done by the averaging of cross-sections obtained by nuclear models with weights proportional to the predictive ability of each model. Neither new algorithms implemented in codes nor new fittings of model parameters can guarantee the best description of experimental data for all nuclei and incident energies (see examples in Ref.23). The question about the predictive power of different models is still open especially for recoil spectra calculations<sup>5</sup>. For this reason the average value of  $\sigma_{d,non}$  presented in Tables II-V has been obtained using equal weights for all models.

TABLE IV. Displacement cross-sections (b) for nonelastic interactions of 1 GeV- protons with <sup>184</sup>W. The nonelastic cross-section is equal to 1.659 b.

Nuclear model	BCA-MD	NRT
Bertini/Dresner	3620	7650
Bertini/ABLA	3950	8490
ISABEL/Dresner	2690	5910
ISABEL/ABLA	3000	6640
CEM03	3580	7580
INCL4/Dresner	2970	6560
INCL4/ABLA	3280	7280
FLUKA/Dresner	5150	10770
FLUKA/ABLA	5630	12020
CASCADE	3640	7750
Average value	3750 ± 950	8100 ± 1900

TABLE V. Displacement cross-sections (b) for nonelastic interactions of 100 GeV- protons with <sup>184</sup>W. The nonelastic cross-section is equal to 1.712 b.

Nuclear model	BCA-MD	NRT
FLUKA/Dresner	5880	10740
FLUKA/ABLA	8180	16000
Average value	7030	13370

### I.C.2. The use of other approaches for the calculation of the number of defects in irradiated materials

Three various approaches for the evaluation of the number of defects are discussed in this Section: the “constant efficiency” approximation<sup>6-8</sup>, NRT<sup>1,2</sup>, and the LSS model<sup>24</sup>.

The crude evaluation of the displacement cross-section can be done using the “constant efficiency” approximation<sup>6-8</sup>. Results of MD calculations are used up to the maximal energy available in the simulation (see e.g. Table I). Above this energy (20-40 keV) the efficiency of the defect generation is taken to be a constant.

Table VI shows the displacement cross-section  $\sigma_{d,non}$  calculated using the BCA-MD approach and the “constant

efficiency” approximation for <sup>184</sup>W. In the last case, the  $\eta$  value was taken equal to 0.26 at the  $T_{dam}$  above 31 keV. At energies below 31 keV Eq.(5) was used to get the number of defects generated. Values of  $\sigma_{d,non}$  shown in Table VI were obtained by the averaging of results of calculations with different nuclear models (see examples in Tables II-V).

One can see that the assumption about the constant efficiency results in 30-50 % lower values of  $\sigma_{d,non}$  comparing with BCA-MD (Table VI). The “constant efficiency” hypothesis is in the contradiction with measurements from Ref.25 showing the relatively high values of  $\eta$  at intermediate ion energies compared with the MD simulation in 20-40 keV region.

TABLE VI. Displacement cross-sections (b) for nonelastic proton interactions with <sup>184</sup>W. Calculations were performed using the BCA-MD approach and the “constant efficiency” approximation. Data were obtained by averaging of results of calculations performed using different nuclear models.

Proton energy	BCA-MD	MD below 31 keV, constant $\eta$ value above
10 MeV	36.9	25.7
20 MeV	218	143
30 MeV	340	232
50 MeV	505	355
70 MeV	630	436
100 MeV	788	532
150 MeV	997	651
300 MeV	1570	974
600 MeV	2630	1540
1 GeV	3750	2100
2 GeV	5070	2670
10 GeV	7100	3560
50 GeV	7410	3670
100 GeV	7030	3480

At high energies of ions the number of defects evaluated using NRT formulas<sup>1,2</sup> differs from one calculated by the LSS approach<sup>24</sup> with the accurate consideration of the energy dependence of electronic and nuclear losses in materials<sup>26</sup>. The number of defects is calculated as follows

$$v(T) = \frac{0.8}{2E_d} \int_0^{E_0} \frac{(dE/dx)_{dam}}{(dE/dx)_{el} + (dE/dx)_n} dE, \quad (7)$$

where  $E_0$  is the primary ion energy,  $(dE/dx)_{el}$  is the electronic stopping power and  $(dE/dx)_n$  is the specific energy loss for the elastic scattering (nuclear loss) and  $(dE/dx)_{dam}$  is the specific energy loss for the damage production:

$$(dE/dx)_{\text{dam}} = n_0 \int_{E_d}^{T_{\text{max}}} (d\sigma(E, T)/dT) T_{\text{dam}}(T) dT \quad (8)$$

In the present work the electronic and nuclear stopping power in Eq.(7) was calculated using the SRIM code<sup>27</sup>. The value of  $d\sigma/dT$  from Eq.(8) was taken from Ref.13, The  $T_{\text{dam}}$  was evaluated according to Refs.1,2.

The displacement cross-section  $\sigma_{\text{d,non}}$  calculated using Eq.(7),(8) and the NRT formulas for  $^{184}\text{W}$  is shown in Table VII. It is seen that the nonelastic displacement cross-section predicted by Eq.(7),(8) with the accurate consideration of electronic and nuclear losses results in higher values of  $\sigma_{\text{d,non}}$  comparing with NRT and other approaches. It increases the difference between calculations and experimental data (Section III).

TABLE VII. Displacement cross-sections (b) for nonelastic proton interactions with  $^{184}\text{W}$ . Calculations were performed using LSS model with correct electronic and nuclear stopping power and NRT model. See other comments to Table VI.

Proton energy	LSS	NRT
10 MeV	110	99.7
20 MeV	600	550
30 MeV	975	894
50 MeV	1500	1370
70 MeV	1850	1680
100 MeV	2280	2050
150 MeV	2830	2500
300 MeV	4330	3750
600 MeV	7090	5940
1 GeV	10140	8060
2 GeV	13970	10270
10 GeV	20110	13680
50 GeV	21140	14100
100 GeV	20120	13370

### III. COMPARISON WITH EXPERIMENTAL DATA

Experimental data for copper and tungsten are available at proton incident energies 1.1 and 1.94 GeV<sup>28</sup>. At low proton energies there are data derived by Jung<sup>29,30</sup> from experimental electron, light ion, and neutron damage rates.

Table VIII and IX show the total displacement cross-section ( $\sigma_{\text{d,el}} + \sigma_{\text{d,non}}$ ) calculated for copper irradiated with 1.1 and 1.94 GeV protons<sup>10</sup>. The elastic component of the cross-section has been obtained as described in Section II.

Table X and XI shows the total displacement cross-section obtained for tungsten irradiated with 1.1 and 1.94 GeV protons.

TABLE VIII. Total displacement cross-section (b) (the sum of elastic and nonelastic components) for natural copper irradiated with 1.1 GeV protons<sup>10</sup>. The elastic displacement cross-sections  $\sigma_{\text{d,el}}$  calculated by BCA-MD is equal to 191.3 b and by NRT is 291.9 b.

Nuclear model	BCA-MD	NRT
Bertini/Dresner	2170	3890
Bertini/ABLA	2360	4260
CEM03	2180	3890
INCL4/Dresner	2590	4620
INCL4/ABLA	2750	4920
FLUKA/Dresner	2790	5190
FLUKA/ABLA	3090	5790
CASCADE	2290	4140
Average value	2530 ± 330	4590 ± 680
Measured value <sup>28</sup>	1440	

TABLE IX. Total displacement cross-section (b) (the sum of elastic and nonelastic components) for natural copper irradiated with 1.94 GeV protons<sup>10</sup>. The elastic displacement cross-sections  $\sigma_{\text{d,el}}$  calculated by BCA-MD is equal to 191.4 b and by NRT is 291.8 b.

Nuclear model	BCA-MD	NRT
Bertini/Dresner	1940	3420
Bertini/ABLA	2170	3870
CEM03	1880	3270
INCL4/Dresner	2510	4470
INCL4/ABLA	2660	4760
FLUKA/Dresner	2550	4710
FLUKA/ABLA	2860	5380
CASCADE	2210	3970
Average value	2350 ± 350	4230 ± 730
Measured value <sup>28</sup>	1830	

Displacement cross-section for tungsten were derived in Ref.27 from experimental data using the Frenkel pair resistivity equal to 14  $\mu\Omega$  m (Ref.31). This value seems questionable taking into account the later analysis<sup>30,32,33</sup>, which gives  $\rho_{\text{FP}} = 27 \pm 6 \mu\Omega$  m. Displacement cross-sections recovered using both these values (14 and 27  $\mu\Omega$  m) are shown in Table X,XI.

There is a rather big difference between measured displacement cross-sections and  $\sigma_{\text{d}}$  calculated using the NRT model (Tables VIII-XI). The agreement with cross-sections obtained from BCA-MD calculations is better.

Fig.5 and Fig.6 show the total displacement cross-section obtained for copper and tungsten at proton incident energies from several keV to 100 GeV. Displacement cross-sections for nonelastic proton interactions included in  $\sigma_{\text{d}}$  were obtained by averaging of  $\sigma_{\text{d,non}}$  values calculated using different nuclear models.

TABLE X. Total displacement cross-section ( $\sigma$ ) (the sum of elastic and nonelastic components) for natural tungsten irradiated with 1.1 GeV protons. The elastic displacement cross-sections  $\sigma_{d,el}$  calculated by BCA-MD is equal to 109 b and by NRT is 164 b.

Nuclear model	BCA-MD	NRT
Bertini/Dresner	3900	8060
Bertini/ABLA	4390	9270
CEM03	3930	8160
INCL4/Dresner	3180	6900
INCL4/ABLA	3510	7670
FLUKA/Dresner	5450	11240
FLUKA/ABLA	6010	12680
CASCADE	3890	8160
Average value	$4280 \pm 970$	$9020 \pm 1970$
Measured value <sup>28</sup> original	4715 at $\rho_{FP} = 14 \mu\Omega$ m (Ref.31)	
Measured value <sup>28</sup> corrected	2445 at $\rho_{FP} = 27 \mu\Omega$ m (Refs.30,32,33)	

TABLE XI. Total displacement cross-section ( $\sigma$ ) (the sum of elastic and nonelastic components) for natural tungsten irradiated with 1.94 GeV protons. The elastic displacement cross-sections  $\sigma_{d,el}$  calculated by BCA-MD is equal to 124 b and by NRT is 200 b.

Nuclear model	BCA-MD	NRT
Bertini/Dresner	4430	8710
Bertini/ABLA	5350	10860
CEM03	4990	9830
INCL4/Dresner	3580	7520
INCL4/ABLA	4020	8550
FLUKA/Dresner	6550	12780
FLUKA/ABLA	7550	15300
CASCADE	4550	9300
Average value	$5130 \pm 1330$	$10360 \pm 2560$
Measured value <sup>28</sup> original	7895 at $\rho_{FP} = 14 \mu\Omega$ m (Ref.31)	
Measured value <sup>28</sup> corrected	4094 at $\rho_{FP} = 27 \mu\Omega$ m (Refs.30,32,33)	

#### IV. DISPLACEMENT CROSS-SECTIONS FOR IRON

Displacement cross-sections were calculated for iron taking into account its special interest for various applications.

The recoil energy distribution for elastic scattering has been calculated using Eq.(6) with the screening function from Ref.13 at incident proton energies up to 2.5 MeV, the optical model with parameters from Ref.16 up to the proton energy 50 MeV, the optical potential from Ref.17 up to  $E_p=0.4$  GeV and using the relativistic formula<sup>18</sup>. Effective threshold energy was taken equal to 40 eV.

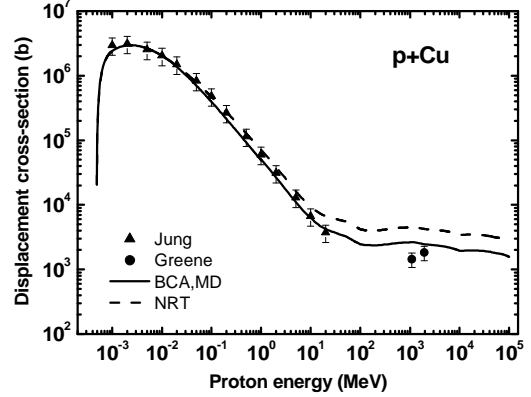


Fig. 5. Total displacement cross-section ( $\sigma_{d,el} + \sigma_{d,non}$ ) for the proton irradiation of copper calculated using the BCA-MD approach<sup>10</sup> (solid line) and the NRT model (dashed line), displacement cross-section obtained by Jung<sup>29,30</sup> (triangle) and data measured in Ref.28 (circle).

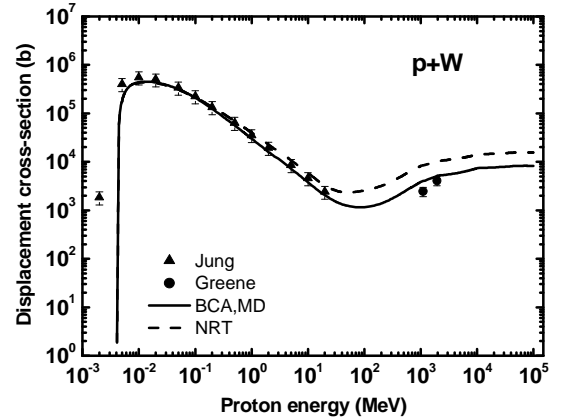


Fig. 6. Total displacement cross-section for the proton irradiation of tungsten calculated using the BCA-MD approach (solid line) and the NRT model (dashed line), displacement cross-section obtained by Jung<sup>29,30</sup> (triangle) and measured in Ref.28 (circle). Data from Ref.28 correspond to  $\rho_{FP} = 27 \mu\Omega$  m.

Displacement cross-sections for nonelastic proton interactions were obtained by averaging of  $\sigma_{d,non}$  values calculated using different nuclear models. The set of models suitable for the  $\sigma_{d,non}$  calculation is different at various proton energies. Examples of appropriate models are shown in Section II and in Ref.10.

Displacement cross-sections calculated for iron and Jung data are shown in Fig.7. Numerical values are given in Table XII. The statistical error of  $\sigma_d$  concerned with the use of various nuclear models is equal to  $\sim 7\%$  at the

proton energy 150 MeV, 12 % for  $E_p = 1$  GeV, 40 % at 50 GeV and ~ 60 % at  $E_p = 100$  GeV.

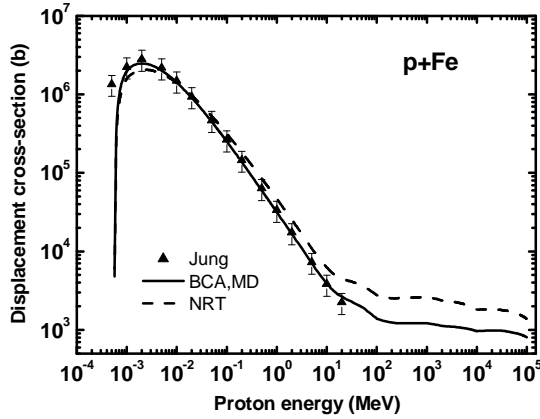


Fig. 7. Total displacement cross-section for the proton irradiation of iron calculated using the BCA-MD approach (solid line) and the NRT model (dashed line), and displacement cross-section obtained by Jung<sup>28,29</sup>.

TABLE XII. Total displacement cross-section (b) for the proton irradiation of natural iron calculated using the BCA-MD approach and the NRT model.

Proton energy	BCA-MD	NRT
570 eV	6020	4780
580 eV	11900	9440
610 eV	$2.89 \times 10^5$	$2.30 \times 10^5$
630 eV	$4.57 \times 10^5$	$3.64 \times 10^5$
650 eV	$6.11 \times 10^5$	$4.86 \times 10^5$
680 eV	$8.18 \times 10^5$	$6.51 \times 10^5$
730 eV	$1.11 \times 10^6$	$8.83 \times 10^5$
810 eV	$1.47 \times 10^6$	$1.17 \times 10^6$
970 eV	$1.92 \times 10^6$	$1.53 \times 10^6$
2.0 keV	$2.48 \times 10^6$	$2.04 \times 10^6$
5.0 keV	$2.01 \times 10^6$	$1.83 \times 10^6$
11 keV	$1.34 \times 10^6$	$1.34 \times 10^6$
19 keV	$9.35 \times 10^5$	$9.95 \times 10^5$
31 keV	$6.53 \times 10^5$	$7.33 \times 10^5$
49 keV	$4.56 \times 10^5$	$5.36 \times 10^5$
76 keV	$3.18 \times 10^5$	$3.89 \times 10^5$
120 keV	$2.15 \times 10^5$	$2.75 \times 10^5$
190 keV	$1.44 \times 10^5$	$1.91 \times 10^5$
290 keV	98200	$1.35 \times 10^5$
430 keV	68600	96900
640 keV	47600	69000
950 keV	33000	48900
1.4 MeV	23100	34800

TABLE XII continued

Proton energy	BCA-MD	NRT
2.1 MeV	15800	24200
3.5 MeV	9910	15300
5.5 MeV	6480	10100
8.5 MeV	4430	7010
10 MeV	3910	6270
15 MeV	2990	4920
20 MeV	2660	4540
30 MeV	2330	4170
40 MeV	2100	3900
50 MeV	1960	3720
75 MeV	1610	3140
100 MeV	1390	2750
150 MeV	1290	2600
200 MeV	1240	2530
300 MeV	1220	2550
600 MeV	1220	2610
1 GeV	1210	2610
2 GeV	1120	2380
5 GeV	1060	2160
10 GeV	962	1810
20 GeV	984	1820
50 GeV	925	1670
75 GeV	873	1540
100 GeV	803	1380

## V. CONCLUSIONS

Displacement cross-sections were obtained for iron, copper, and tungsten irradiated with protons at energies from several keV up to 100 GeV using the binary collision approximation model and results of molecular dynamics simulations. Recoil energy distributions were calculated using various approaches including the model for screened Coulomb scattering, the optical model and the intranuclear cascade evaporation model. Resulting displacement cross-sections are in better agreement with available experimental data than cross-sections calculated by the NRT model.

## REFERENCES

1. M. J. NORGETT, M. T. ROBINSON, and I. M. TORRENS, *Nucl. Eng. Des.*, **33**, 50 (1975).
2. M. T. ROBINSON, *J. Nucl. Mater.*, **216**, 1 (1994).
3. C. H. M. BROEDERS and A. YU. KONOBEYEV, *J. Nucl. Mater.*, **328**, 197 (2004).
4. C. H. M. BROEDERS and A. YU. KONOBEYEV, *J. Nucl. Mater.*, **336**, 201 (2005).
5. C. H. M. BROEDERS, A. YU. KONOBEYEV, and C. VILLAGRASA, *J. Nucl. Mater.*, **342**, 68 (2005).
6. R. E. STOLLER and L. R. GREENWOOD, *J. Nucl. Mater.*, **271&272**, 57 (1999).

7. R. E. STOLLER, *Nucl. Eng. Des.*, **195**, 129 (2000).
8. M.J. CATURLA, T. DIAZ DE LA RUBIA, M. VICTORIA, R. K. CORZINE, M. R. JAMES, and G. A. GREENE, *J. Nucl. Mater.*, **296**, 90 (2001).
9. C. H. M. BROEDERS, A. YU. KONOBEYEV, and K. VOUKELATOU, *IOTA - a Code to Study Ion Transport and Radiation Damage in Composite Materials*, FZKA 6984 (2004); <http://bibliothek.fzk.de/zb/berichte/FZKA6984.pdf>
10. A. YU. KONOBEYEV, C. H. M. BROEDERS, and U. FISCHER, "Calculation of Displacement Cross Sections at Intermediate and High Energies of Primary Particles Using Results of Molecular Dynamics Simulations", *Proc. Int. Conference for Nuclear Science and Technology*, Nice, April 22-27, 2007.
11. C. H. M. BROEDERS and A. YU. KONOBEYEV, "Investigation of Radiation Damage Rates in a LWR Vessel Using Results of Molecular Dynamics Simulations", *Proc. Workshop on Structural Materials for Innovative Nuclear Systems (SMINS)*, Karlsruhe, June 4-6, 2007.
12. W. ECKSTEIN, *Computer Simulation of Ion-Solid Interactions*, Springer-Verlag (1991).
13. K. B. WINTERBON, P. SIGMUND, and J. B. K. SANDERS, "Spatial Distribution of Energy Deposited by Atomic Particles in Elastic Collisions", *K. Dan. Vidensk. Selsk. Mat. Fys. Medd.* **37**, 14 (1970).
14. A. F. BURENKOV, F. F. KOMAROV, M. A. KUMAHOV, and M. M. TEMKIN, *Spacial Distribution of Energy Deposited in Atomic Collision Cascades in Matter*, Energoatomizdat. Moscow. (1985).
15. U. LITTMARK and J. F. ZIEGLER, *Handbook of Range Distributions*, Pergamon Press (1985).
16. A. J. KONING and J. P. DELAROCHE, *Nucl. Phys.*, **A713**, 231 (2003).
17. D. G. MADLAND, "Progress in the Development of Global Medium-Energy Nucleon-Nucleus Optical Model Potentials", *Proc. of the Specialists' Meeting on the Nucleon Nucleus Optical Model up to 200 MeV*, Bruyères-le-Chatel, November 13-15, 1996 p.129; <http://www.nea.fr/html/science/om200/>
18. INSOO JUN, *IEEE Trans. Nucl. Sci.*, **48**, 162 (2001).
19. J. S. HENDRICKS, G. W. MCKINNEY, J. W. DURKEE, et al., LA-UR-06-7991 Dec.7 (2006).
20. V. S. BARASHENKOV, *Comp. Phys. Comm.* **126**, 28 (2000).
21. C. H. M. BROEDERS, A. YU. KONOBEYEV, YU. A. KOROVIN, and V. N. SOSNIN, *DISCA - Advanced Intranuclear Cascade Cluster Evaporation Model Code System for Calculation of Particle Distributions and Cross Sections at Emitted Particles in Nuclear Reactions at Intermediate Energies*, Forschungszentrum Karlsruhe, FZKA 7221, (2006); <http://bibliothek.fzk.de/zb/berichte/FZKA7221.pdf>
22. C. H. M. BROEDERS and A. YU. KONOBEYEV, *Nucl. Instr. Meth. Phys. Res.*, **B234**, 387 (2005).
23. YU. KOROVIN, U. FISCHER, A. KONOBEYEV, A. NATALENKO, G. PILNOV, A. STANKOVSKIY and A. TIKHONENKO "Evaluation of Activation Nuclear Data in the Energy Region 150 MeV to 1 GeV", *Proc. Int. Conference for Nuclear Science and Technology*, Nice, April 22-27, 2007.
24. J. LINDHARD, M. SCHARFF, and H. E. SCHIOTT, "Range Concepts and Heavy Ion Ranges", *K. Dan. Vidensk. Selsk. Mat. Fys. Medd.* **37**, 14 (1970).
25. A. DUNLOP, D. LESUEUR, P. LEGRAND, and H. DAMMAK, *Nucl. Instr. Meth. Phys. Res.*, **B90**, 330 (1994).
26. A. YU. KONOBEYEV, YU. V. KONOBEYEV, and YU. A. KOROVIN, *J. Nucl. Sci. Technol.*, **Suppl. 2**, 1236 (2002).
27. J. F. ZIEGLER, *Particle Interactions with Matter*, <http://www.srim.org>
28. G. A. GREENE, C. L. SNEAD JR., C. C. FINFROCK, A. L. HANSON, M. R. JAMES, W. F. SOMMER, E. J. PITCHER, and L. S. WATERS, in: *Proc. Sixth International Meeting on Nuclear Applications of Accelerator Technology (AccApp'03)*, p. 881, San Diego, June 1-5, 2003, American Nuclear Society, La Grande Park, Illinois (2004).
29. P. JUNG, *J. Nucl. Mater.*, **117**, 70 (1983).
30. P. JUNG, "Production of Atomic Defects in Metals", *Landolt-Börnstein, Group III: Crystal and Solid State Physics*, Ed. H.Ullmaier, Springer-Verlag, Berlin, **25**, 1 (1991).
31. P. LUCASSON, *Fundamental Aspects of Radiation Damage in Metals*, Eds. M.T. Robinson, F.W. Young, Jr., vol. 1 (1976), p.42 (CONF-75-1006-P1, US ERDA, Washington, DC, 1975)
32. O. DIMITROV and C. DIMITROV, *Rad. Eff.*, **84**, 117 (1985).
33. G. WALLNER, M. S. ANAND, L. R. GREENWOOD, M. A. KIRK, W. MANSEL, and W. WASCHKOWSKI, *J. Nucl. Mater.*, **152**, 146 (1988).